SUBSURFACE ICE STRUCTURE ANALYSIS WITH LONGER WAVELENGTH SAR TOMOGRAPHY

Francesco Banda[1], **Jørgen Dall**[2], **Stefano Tebaldini**[1], **and Fabio Rocca**[1]

[1]*Politecnico di Milano, Dipartimento di Elettronica, Informazione e Bioingegneria*
[2]*Technical University of Denmark, National Space Institute*

ABSTRACT

Given the extreme importance of monitoring ice sheets with remote sensing instruments in order to predict their interactions with the environment, the ESA IceSAR 2012 campaign was performed in south-west Greenland in the framework of BIOMASS activities. The objective was to assess the capability of longer wavelength SAR to retrieve information about ice flow and structure. In the present paper first results from processing of tomographic data for subsurface ice structure mapping are presented. The extent of signal penetration has been found to be of about 20-60 m, conditional on the different glacier zone investigated.

Key words: Synthetic aperture radar, SAR tomography, Glaciology, Ice thickness and structure, BIOMASS.

1. INTRODUCTION

The dramatic increase of the melting of ice sheets over the last decades demands for detailed large scale analyses of glaciological features such as mass balance, structure and dynamics. This can be achieved through remote sensing instruments and the forthcoming Earth Explorer mission BIOMASS, selected in May 2013 [1], represents a very important opportunity for future investigations, due to the potentiality of P-band to penetrate the illuminated medium.
The aim of the ESA IceSAR campaign performed in 2012 [2] was to assess the capabilities of P-band SAR to provide suitable products of ice flow and subsurface, given also the promising results reported in literature on the retrieval of information about the structure of ice with SAR and radar sounding [3, 4, 5]. Longer wavelength tomographic SAR, in addition, provides a direct access to the volumetric structure of complex media and separation of the scattering mechanisms in elevation within the radar resolution cell (as witnessed by recent results obtained in the study of forested areas, which is the primary objective of BIOMASS, [6, 7]). Airborne multibaseline and fully polarimetric SAR data were acquired by flying POLARIS radar [2, 5] over different test sites in Greenland, in order to carry out the investigations.
The first results from tomographic data processing regarding the volumetric structure of ice are here discussed. Penetration of the radar signal in the upper layers of ice subsurface and evidence of a morphological structure have been observed. Moreover separation of the ice volume from the surface has been achieved in one of the investigated sites applying Algebraic Synthesis [6] to the fully polarimetric dataset available.

2. TEST SITES AND FLIGHTS

The activities focused on the K-transect in south-west Greenland, located east of Kangerlussuaq at 67° N, on the Russell glacier [2, 8]. This area, which comprises eight measurement sites, is characterized by relatively high ablation and low accumulation and it has a smooth topography that decreases from the inner part to the edge of the ice sheet. Airborne P-band (435 MHz) radar POLARIS, reconfigurable from sounder to SAR capability, was used to acquire the data.
Two of the sites in particular have been investigated with tomography: SHR and S10. The two sites belong to different ice zones: SHR site (50° W, average altitude approximately 700 m) is in the ablation zone of the glacier, whereas S10 site (47° W, average altitude approximately 1850 m) is located in the accumulation area, in particular in the percolation zone. This implies a notable difference in the physical structure of the ice between the two sites [9]. The ablation zone is characterized by the presence of meltwater and features like streams and lakes may be found. The percolation zone is characterized by localized percolations from the surface during melting without becoming entirely wet. The subsequent refreezing of the percolating meltwater into snow layers forms ice pipes and lenses.
Multibaseline HH polarization acquisitions explicitly designed for tomography were gathered by flying POLARIS repeatedly on a nominally straight track at SHR site, in May and June. In this case baselines correspond to the deviations from the planned track caused by the achievable flight control precision and impact of the wind. With this choice almost unambiguous imaging lacking a-priori knowledge of the effective penetra-

Proc. 'ESA Living Planet Symposium 2013', Edinburgh, UK
9–13 September 2013 (ESA SP-722, December 2013)

tion depth and wind conditions is guaranteed. Fully polarimetric multibaseline data were additionally acquired in order to perform polarimetric and interferometric analyses. Multibaseline fully polarimetric data were acquired also at S10 site, in April. Although tomographic analysis has been carried out also for S10 site, the experiment at S10 was not designed for this purpose. Thus, in this case only a few sparse baselines are available. The vertical resolution varies globally from 10 m to 300 m both at SHR and S10, with greater baselines on average at S10.

3. TOMOSAR PROCESSING

Along track focusing of Level 0 raw products was achieved with time domain back-projection algorithm [10]. The algorithm takes as input topographic information and navigation data, in order to account for the deviations of the real trajectory from the planned straight track. Moreover, provided that correct information about topography is available, automatic co-registration of the data stack is achieved. Eight passes for SHR site and four passes for S10 site were processed.

After along track focusing, tomographic processing has been applied. Tomographic SAR relies on the formation of a bi-dimensional synthetic aperture from multiple acquisitions of the same scene along parallel flight lines. In this way different vertical wavenumbers of the object under investigation are illuminated. The reflectivity profile of the scene in the vertical direction and SAR multibaseline data form a Fourier pair and the former can be reconstructed by simply Fourier transforming the data along the baseline direction [11]. However, two important issues must be considered in the processing. First of all, the resolution is limited from the total baseline aperture in the vertical direction. Moreover, the actual flight tracks always depart from the planned ones because of the limited stability of the aircraft and weather conditions. This causes an uneven sampling of the aperture, with consequent aliasing of the resulting image due to the presence of strong grating lobes. SAR tomography is thus more often recast as a spectral estimation problem and super-resolution techniques like Capon spectral estimator are applied [12]. Prior to tomography, data need to be also phase calibrated, in order to remove platform positioning errors that prevent from correct focusing (for the details about the calibration procedure applied to the data here discussed see [13]). Tomographic data focusing has been achieved by neglecting the change of velocity due to the propagation of the wave into the ice volume. This fact has to be taken into account for the interpretation of the tomographic results, since the actual depth of the observable subsurface structures need to be re-scaled considering a proper dielectric permittivity for ice.

Algebraic Synthesis was introduced in [6] for the decomposition of second-order statistics of multibaseline fully polarimetric data into different scattering mechanisms. In [6, 7] the decomposition was applied to data of forested areas to obtain two scattering mechanisms, one associated with volumetric backscattering and the other one associated with the ensemble of ground-locked scattering mechanisms. The same approach is here applied to ice data from S10 site to assess whether it is possible to separate subsurface ice volume from surface or not.

4. SUBSURFACE ANALYSIS

4.1. SHR

In Figure 1 the magnitude of the coherence between all the processed flights is represented for SHR. The *nm-th* entry of the matrix represents the coherence magnitude between flight n an flight m for the entire scene focused in the ground range-azimuth plane. Below the diagonal real coherences are shown, above the diagonal simulated data with 50 m penetration and an exponential extinction profile are represented. Although a loose decorrelation pattern can be identified (data are ordered according to their acquisition time), coherence is found to be overall quite high, in particular higher than the corresponding simulated values. This indicates the prevalence of scattering from a superficial mechanism, with no relevant volumetric decorrelation.

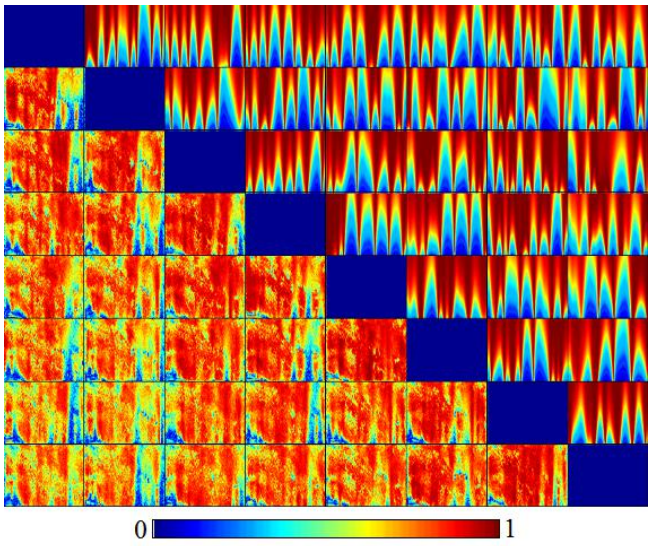

Figure 1. Interferometric coherence magnitudes at SHR (May 2012, similar results are found for June 2012). Lower left panels are relative to real data. Upper right panels were obtained by simulating an exponential vertical profile with characteristic penetration of 50 m. Images are sorted by their acquisition time.

The result is very consistent with the intense melting recorded in Greenland in 2012 [14, 15], due to the fact that meltwater inhibits the penetration of the radar waves. It is worth remarking, however, that this is in part due to the coarse vertical resolution at SHR, since the experiment was conceived so as to guarantee unambiguous imaging for a penetration of hundred of meters. In Figure 2 tomographic sections obtained with Capon beamforming are shown for the estimated ice/air interface (which

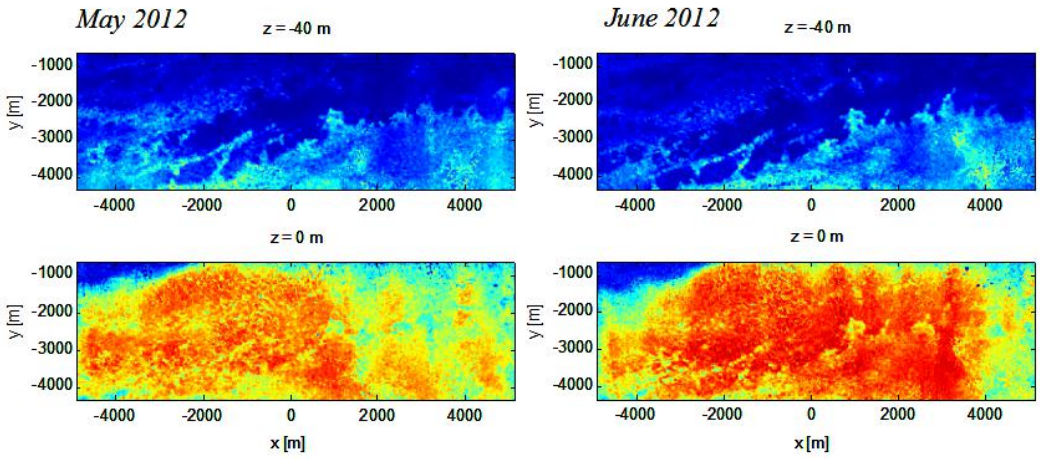

Figure 2. Capon tomograms of SHR in May (left) and June (Right). x, y and z coordinates are referred to azimuth, ground range and elevation respectively. Lower panels represent the tomographic sections relative to the estimated ice/air interface. Upper panels represent tomographic sections at 40 m below the estimated interface. Values are scaled between 0 (blue) and 1 (red) for representation. Focusing is achieved by neglecting the change of velocity due to the propagation of the wave into the ice volume.

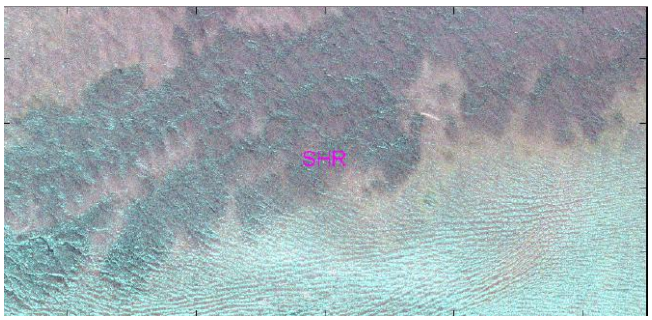

Figure 3. SHR June data, polarimetric image. PolSAR color map: HV=red, HH=green, VV=blue.

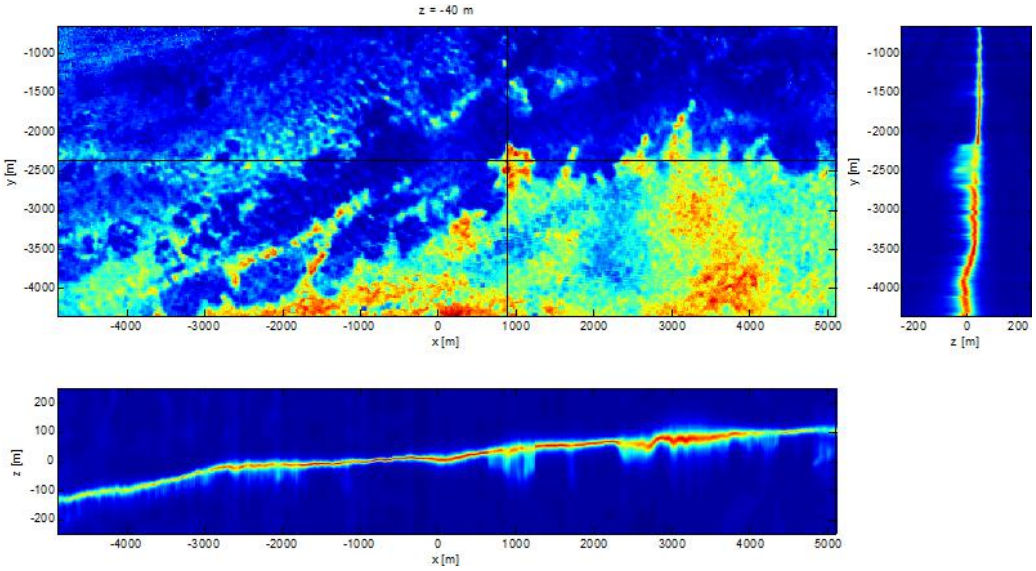

Figure 4. Capon tomogram of SHR June at -40 m elevation (central panel) along with a profile in the ground range-elevation plane (on the right) and a profile in the azimuth-elevation plane (to the bottom), highlighted on the image with black lines. Focusing is achieved by neglecting the change of velocity due to the propagation of the wave into the ice volume.

is indicated as 0 m elevation) and at 40 m below the surface. It can be observed how clear morphological features appear at subsurface, even though the scattering is mostly superficial. It is also worth noting how the signal strength at 0 m is higher in June, consistently with the increased melt rate. In Figure 3 the lexicographic representation of SHR June data is shown. The polarimetric image highlights significant contributions from the cross-pol channel, some of which match the locations of Figure 2 at -40 m in which morphological features appear. This fact is consistent with the physics of volumetric scattering and corroborates the hypothesis of shallow penetration of the radar wave into the ice. In Figure 4 the June tomographic section at -40 m is shown along with the two profiles corresponding to the black lines in the central panel: a profile in the ground range-elevation plane (on the right) and a profile in the azimuth-elevation plane (to the bottom). Observing the two profiles it clearly appears how significant penetration changes between nearby areas, although shallow, occur.

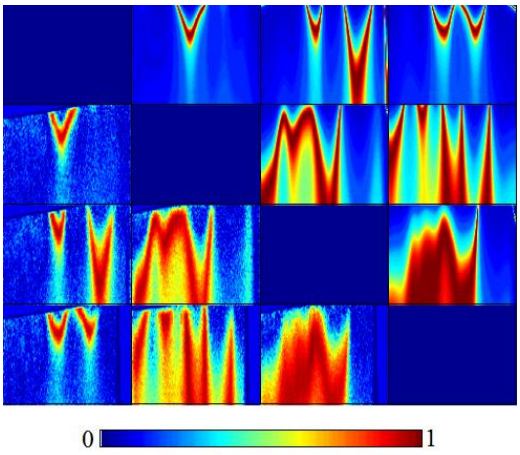

Figure 5. Interferometric coherence magnitudes at S10. Lower left panels are relative to real data. Upper right panels were obtained by simulating an exponential vertical profile with characteristic penetration of 50 m.

4.2. S10

In Figure 5 the coherence values are represented for S10 site. In this case agreement between real and simulated values is very good, indicating clear volumetric decorrelation. In Figure 6 tomographic profiles for S10 are shown. A clear interpretation of the results is partly hindered from the irregularity of the impulse response in the elevation plane. This is because the four S10 acquisitions were not designed for tomography. Nonetheless a difference between HH and HV channels indicating possible volumetric scattering is clearly observable. Separation of volume and surface has been obtained from the whole fully polarimetric dataset using Algebraic Synthesis. In Figure 6 a result of the decomposition is shown for the most coherent surface and most distributed volume [7]. A situation similar to that of forested scenarios is observed: a strong and very localized scattering mechanism can be identified as a first scattering contribution and a distributed scattering mechanism appears localized beneath the surface (rather than above as in the case of forests). A very good similarity is observed between HH data and surface mechanism and between HV data and volume, consistently with the polarimetric behavior of the two physical mechanisms assumed.

5. SCATTERING DEPTH

5.1. SHR

A quantitative assessment of the scattering depth has been done at SHR with the MUSIC spectral estimator [12, 16]. The upper and lower boundaries of the ice layer are estimated as corresponding to the locations of the two highest peaks in the vertical spectrum. The average penetration depth obtained is on the order of 40 m assuming propagation in air, which scales down to about 20 m considering ice propagation velocity (in this case a dielectric permittivity $\varepsilon_r \cong 3$ has been assumed for ice). The resulting penetration map is shown in Figure 7.

5.2. S10

For S10 a rough estimate can be obtained from the thickness of volume tomograms resulting from Algebraic Synthesis (Figure 6, lower right panel). In this case the maximum penetration depth observed is on the order of 100 m in air, corresponding to about 60 m in ice.

6. CONCLUSIONS

In this paper investigation of the subsurface structure of ice with tomographic SAR has been discussed. First results from processing of IceSAR 2012 tomographic data have been presented.
Focusing in the vertical plane has been achieved with Capon non-parametric spectral estimator. The super-resolution properties of Capon estimator allow to overcome the insufficient resolving power of the traditional Fourier beamforming with respect to the entity of the penetration phenomena observed. In addition a much better mitigation of the sidelobes is obtained.
At SHR site the scattering has been found to be mostly superficial, especially in June because of the increased melt rate. Nonetheless a clear morphological structure has been observed at subsurface. A possible explanation could be attributed to some meltwater percolation into subsurface layers. Further analyses will be devoted to investigate this point.
In the case of S10 data relevant volumetric decorrelation has been found and polarimetric/tomographic approaches have been used to decompose the data into two scattering

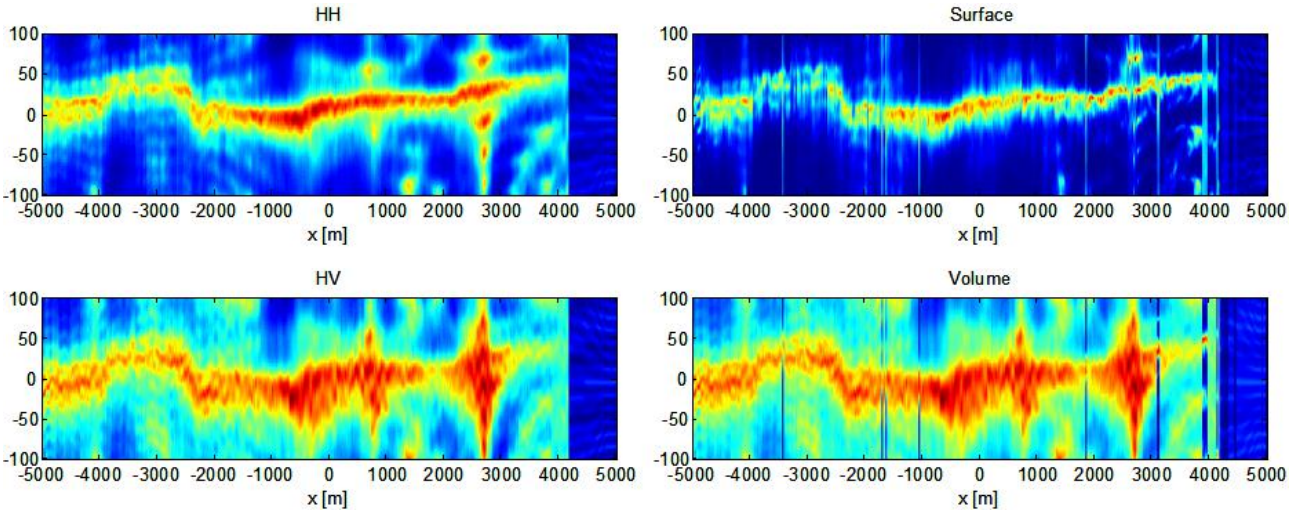

Figure 6. S10 data. Capon tomogram from HH data (upper left panel), HV data (lower left panel) and results of Algebraic Synthesis: upper right panel is the superficial scattering mechanism, lower right panel is the volume. The volumetric contribution is clearly distributed at subsurface. Focusing is achieved by neglecting the change of velocity due to the propagation of the wave into the ice volume.

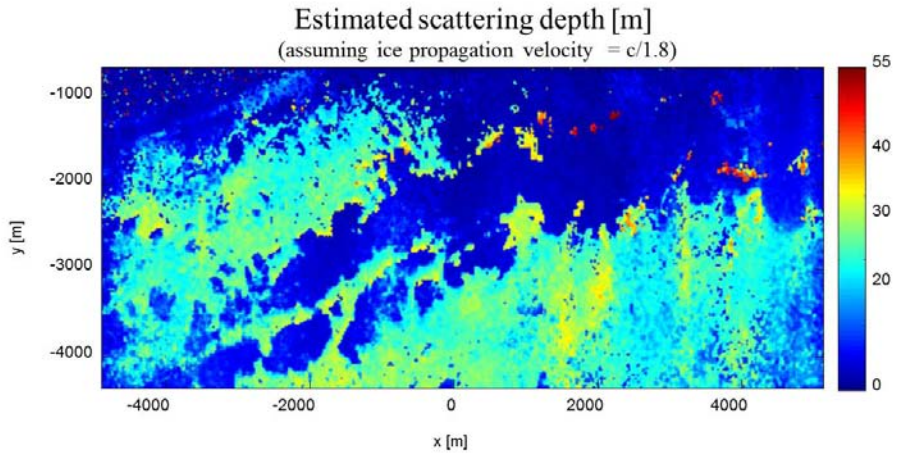

Figure 7. Penetration depth obtained as the difference between the upper and lower ice boundaries estimated by the MUSIC algorithm, SHR May.

mechanisms, namely surface and subsurface.
Scattering depth has been quantified using MUSIC parametric spectral estimator for SHR and from the thickness of the tomograms of the volumetric scattering mechanism for S10. The resulting penetration depth is on the order of 40 m for SHR and 100 m for S10 assuming propagation in air, which scales down to about 20 m for SHR and 60 m for S10 taking into account the velocity of propagation in ice.

REFERENCES

1. "ESA Press Release N 13-2013: ESAs next Earth Explorer satellite," .

2. J. Dall, U. Nielsen, A. Kusk, S.S. Kristensen, and R.S.W. van de Wal, "Ice flow mapping with P-band SAR," in *Geoscience and Remote Sensing Symposium (IGARSS), 2013 IEEE International*, July 2013.

3. J.J. Sharma, I. Hajnsek, K.P. Papathanassiou, and A. Moreira, "Polarimetric Decomposition Over Glacier Ice Using Long-Wavelength Airborne PolSAR," *Geoscience and Remote Sensing, IEEE Transactions on*, vol. 49, no. 1, pp. 519 –535, Jan. 2011.

4. Xiaoqing Wu, K.C. Jezek, E. Rodriguez, S. Gogineni, F. Rodriguez-Morales, and A. Freeman, "Ice Sheet Bed Mapping With Airborne SAR Tomography," *Geoscience and Remote Sensing, IEEE Transactions on*, vol. 49, no. 10, pp. 3791 –3802, Oct. 2011.

5. J. Dall, S.S. Kristensen, V. Krozer, C.C. Hernandez, J. Vidkjr, A. Kusk, J. Balling, N. Skou, S.S. Sbjrg, and E.L. Christensen, "ESA'S POLarimetric Airborne Radar Ice Sounder (POLARIS): design and first results," *Radar, Sonar Navigation, IET*, vol. 4, no. 3, pp. 488 –496, June 2010.

6. S. Tebaldini, "Algebraic Synthesis of Forest Scenarios From Multibaseline PolInSAR Data," *Geoscience and Remote Sensing, IEEE Transactions on*, vol. 47, no. 12, pp. 4132 –4142, Dec. 2009.

7. S. Tebaldini and F. Rocca, "Multibaseline Polarimetric SAR Tomography of a Boreal Forest at P- and L-Bands," *Geoscience and Remote Sensing, IEEE Transactions on*, vol. 50, no. 1, pp. 232–246, 2012.

8. R.S.W. Van De Wal, W. Greuell, M.R. Van Den Broeke, C.H. Reijmer, and J. Oerleman, "Surface mass-balance observations and automatic weather station data along a transect near Kangerlussuaq, West Greenland," *Annals of Glaciology*, vol. 42, pp. 311 –316, Aug. 2005.

9. W.S.B. Paterson, *The Physics of Glaciers*, Butterworth-Heinemann, Elsevier, Third edition, 1994.

10. L. M H Ulander, H. Hellsten, and G. Stenstrom, "Synthetic-aperture radar processing using fast factorized back-projection," *Aerospace and Electronic Systems, IEEE Transactions on*, vol. 39, no. 3, pp. 760–776, 2003.

11. A. Reigber and A. Moreira, "First demonstration of airborne SAR tomography using multibaseline L-band data," *Geoscience and Remote Sensing, IEEE Transactions on*, vol. 38, no. 5, pp. 2142 –2152, Sep 2000.

12. F. Gini, F. Lombardini, and M. Montanari, "Layover solution in multibaseline SAR interferometry," *Aerospace and Electronic Systems, IEEE Transactions on*, vol. 38, no. 4, pp. 1344 – 1356, Oct 2002.

13. S. Tebaldini, M. Mariotti d'Alessandro, F. Banda, and C. Prati, "Tomographic-quality Phase Calibration via Phase Center Double Localization," in *Geoscience and Remote Sensing Symposium (IGARSS), 2013 IEEE International*, July 2013.

14. "Satellites See Unprecedented Greenland Ice Sheet Surface Melt, NASA News release 12-249 (2012)," .

15. "An intense Greenland melt season: 2012 in review, NSIDC, February 5, 2013," .

16. Petre Stoica, Jian Li, and Xing Tan, "On Spatial Power Spectrum and Signal Estimation Using the Pisarenko Framework," *Signal Processing, IEEE Transactions on*, vol. 56, no. 10, pp. 5109–5119, 2008.